Wavelet analysis of beam-soil structure response for fast moving train

2009 J. Phys.: Conf. Ser. 181 012052

(http://iopscience.iop.org/1742-6596/181/1/012052)

Journal of Physics: Conference Series **181** (2009) 012052 doi:10.1088/1742-6596/181/1/012052

Wavelet analysis of beam-soil structure response for fast moving train

Piotr Koziol[1], Zdzislaw Hryniewicz[1], Cristinel Mares[2]

[1] Koszalin University of Technology
Department of Civil and Environmental Engineering
Sniadeckich 2, 75-453 Koszalin, Poland

[2] Brunel University
School of Engineering and Design
Uxbridge, Middlesex, UB8 3PH, UK

Piotr.Koziol@wbiis.tu.koszalin.pl

Abstract. This paper presents a wavelet based approach for the vibratory analysis of beam-soil structure related to a point load moving along a beam resting on the surface. The model is represented by the Euler-Bernoulli equation for the beam, elastodynamic equation of motion for the soil and appropriate boundary conditions. Two cases are analysed: the model with a half space under the beam and the model where the supporting medium has a finite thickness. Analytical solutions for the displacements are obtained and discussed in relation to the used boundary conditions and the type of considered loads: harmonic and constant. The analysis in time-frequency and velocity-frequency domains is carried out for realistic systems of parameters describing physical properties of the model. The approximate displacement values are determined by applying a wavelet method for a derivation of the inverse Fourier transform. A special form of the coiflet filter used in numerical calculations allows to carry out analysis without loss of accuracy related to singularities appearing in wavelet approximation formulas, when dealing with standard filters and complex dynamic systems.

1. Introduction

The problem analysed in this paper is related to the abatement of vibrations generated by high-speed trains. The investigation of the traffic interaction with the environment plays a significant role in the construction of new tracks and trains [1, 2, 3] and is one of most important subjects of EU research in the area of surface transportation.

Modern high-speed trains move with velocities which increase very dangerously the level of vibrations [4, 5]. The Rayleigh velocity is usually treated as a critical velocity and the theoretical investigations and experimental tests show that the ground vibrations grow significantly when the trains' speed reaches this critical value [6, 7]. Although many results concerning railway tracks built on the surface were described in the literature [3, 6], new analytical and numerical approaches to the problem of vibrations abatement are still needed, with special interest in ground vibration analysis [7, 8, 9].

The type of the load and properties of the supporting layer strongly influence the level of accuracy of numerical approximations of displacement. Two different cases of the same model are presented in

this paper: the first one with a half space under the beam and the second one when the supporting layer has finite thickness. The complexity of solutions is discussed in relation to the velocity and frequency of the load. The level of vibrations generated by the load is computed in the cases of harmonic and constant point loads moving along the beam resting on the surface of viscoelastic medium. The case of the harmonic load is very important for the analysis of surface vibrations generated by moving load and usually shows a strong response of the system for even its small velocities. It does not show any singularities in mathematical formulas and can be effectively solved by using carefully adopted calculation methods. In order to avoid numerical instabilities appearing for some systems of parameters, a wavelet approximation method [10] and a specially chosen coiflet filter [11] are used for derivation of the inverse Fourier transform. This method is very effective for high velocities and high load frequencies and allows to reduce numerical problems for calculations that prevent effective analysis of the system due to the big amount of time needed for calculations [12].

2. A load moving along a beam

An infinitely long beam is resting on viscoelastic surface and the point load is moving along the beam. Two cases are analyzed: finite thickness h of supporting medium (Fig.1) and a half space under the beam (Fig.2).

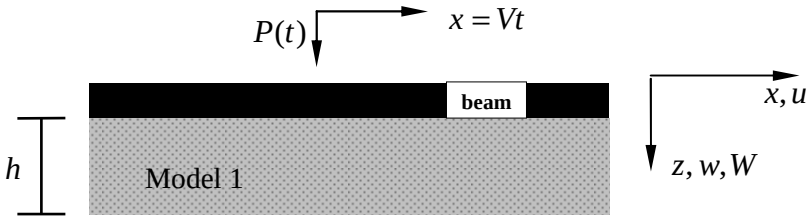

Figure 1: Finite thickness of the medium.

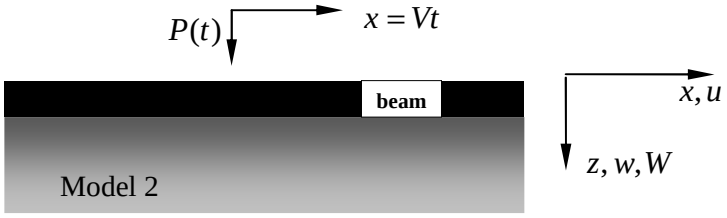

Figure 2: Half space under the beam.

The equation for the vertical motion of the beam can be written as Euler Bernoulli equation:

$$EI\frac{\partial^4 W(x,t)}{\partial x^4}+\rho_B\frac{\partial^2 W(x,t)}{\partial t^2}=P(t)\delta(x-Vt)-a\sigma_{zz}(x,0^+,t) \tag{1}$$

where $W(x,t)$, $\sigma_{zz}(x,z,t)$, $P(t)$, EI, ρ_B, a and $\delta(\cdot)$ are the vertical displacement of the beam, the vertical stress, the vertical point load, the bending stiffness, the mass per unit length of the beam, the thickness of the beam in y direction and the Dirac delta function, respectively.

The motion of the viscoelastic layer can be described by the following elastodynamic Navier's equation:

$$(\lambda+\mu+(\lambda^*+\mu^*)\frac{\partial}{\partial t})\nabla_{xz}(\nabla_{xz}\mathbf{u})+(\mu+\mu^*\frac{\partial}{\partial t})\nabla_{xz}^2\mathbf{u}=\rho\frac{\partial^2\mathbf{u}}{\partial t^2} \quad (2)$$

where $\mathbf{u}(x,z,t)=[u(x,z,t),0,w(x,z,t)]$, ρ and λ, μ are the displacement vector, the mass density of the soil and Lame' constants, respectively. The boundary and continuity conditions are:

$$u(x,0,t)=0, \quad (3)$$

$$w(x,0,t)=W(x,t), \quad (4)$$

$$u(x,h,t)=0,\ w(x,h,t)=0 \text{ (for model 1)} \quad (5a)$$

$$\lim_{z\to\infty}u(x,z,t)=0,\ \lim_{z\to\infty}w(x,z,t)=0 \text{ (for model 2).} \quad (5b)$$

The interpretation of these conditions can be described in the following way: the beam does not move horizontally, the vibrations of the beam and the vertical displacements of the soil at the surface are the same and the radiated waves vanish at $z=h$ (model 1) and at the infinity (model 2). The Fourier transform can be used for obtaining the steady state response of the surface for these systems [4]. The described model presents the system based on the assumptions formulated in [4, 12] where the problem of ground vibrations due to a load moving in a tunnel is investigated for harmonic and constant loads. Accordingly the reformulated equations and conditions lead to the investigation of the soil response for the load moving along the beam resting on the surface similar to the models published in [8, 13, 9] where the main direction of investigation is focused on derivation of critical velocities. One should note that the present paper analyses the two-dimensional model, whereas the analysis in three dimensions would allow to solve the problem in a more general case with y direction and possibly simplify some calculations by introduction of other systems of coordinates.

3. Analytical solution

The formulas for displacements and stress components can be rewritten by using Lame' potentials:

$$u=\frac{\partial\varphi}{\partial x}+\frac{\partial\psi}{\partial z},\ w=\frac{\partial\varphi}{\partial z}-\frac{\partial\psi}{\partial x},\ \sigma_{zz}=\left(\lambda+\lambda^*\frac{\partial}{\partial t}\right)\left(\frac{\partial^2\varphi}{\partial x^2}+\frac{\partial^2\varphi}{\partial z^2}\right)+2\left(\mu+\mu^*\frac{\partial}{\partial t}\right)\left(\frac{\partial^2\varphi}{\partial z^2}-\frac{\partial^2\psi}{\partial x\partial z}\right) \quad (6)$$

Instead of equation (2) one can write two scalar equations:

$$\rho\frac{\partial^2\varphi}{\partial t^2}=\left(\lambda+2\mu+(\lambda^*+2\mu^*)\frac{\partial}{\partial t}\right)\left(\frac{\partial^2\varphi}{\partial x^2}+\frac{\partial^2\varphi}{\partial z^2}\right),\ \left(\mu+\mu^*\frac{\partial}{\partial t}\right)\left(\frac{\partial^2\psi}{\partial x^2}+\frac{\partial^2\psi}{\partial z^2}\right)=\rho\frac{\partial^2\psi}{\partial t^2}. \quad (7)$$

Applying the Fourier transforms

$$\tilde{\tilde{f}}(k,\omega)=\int_{-\infty}^{+\infty}\int_{-\infty}^{+\infty}f(x,t)e^{i(\omega t-kx)}dxdt,\quad f(x,t)=\frac{1}{4\pi^2}\int_{-\infty-\infty}^{+\infty+\infty}\tilde{\tilde{f}}(k,\omega)e^{-i(\omega t-kx)}d\omega dk \quad (8)$$

gives the following representation of the system in the transform domain:

$$(EIk^4-\rho_B\omega^2)\tilde{\tilde{W}}(k,\omega)=\int_{-\infty}^{+\infty}P(t)e^{i(\omega-kV)t}dt-a\tilde{\tilde{\sigma}}_{zz}(k,0^+,\omega) \quad (9a)$$

$$\frac{d^2\tilde{\tilde{\varphi}}}{dz^2}-R_L{}^2\tilde{\tilde{\varphi}}=0,\ \frac{d^2\tilde{\tilde{\psi}}}{dz^2}-R_T{}^2\tilde{\tilde{\psi}}=0 \quad (9b)$$

where $R_L{}^2=k^2-\omega^2/(c_L{}^2-i\omega(\lambda^*+2\mu^*)/\rho)$, $R_T{}^2=k^2-\omega^2/(c_T{}^2-i\omega\mu^*/\rho)$ and c_L, c_T are velocities of the longitudinal and the shear waves in the layer, respectively.

The boundary and continuity conditions (3)-(5) can be rewritten accordingly:

$$\tilde{\tilde{u}}(k,0,\omega)=0,\ \tilde{\tilde{w}}(k,0,\omega)=W(k,\omega),\ \tilde{\tilde{u}}(k,h,\omega)=\tilde{\tilde{w}}(k,h,\omega)=0,$$

$$\lim_{z\to\infty}\tilde{\tilde{u}}(k,z,\omega)=\lim_{z\to\infty}\tilde{\tilde{w}}(k,z,\omega)=0.$$

The solutions for equations (9b) are:

$$\tilde{\tilde{\varphi}} = A_1(k,\omega)e^{R_L z} + A_2(k,\omega)e^{-R_L z},\ \tilde{\tilde{\psi}} = A_3(k,\omega)e^{R_T z} + A_4(k,\omega)e^{-R_T z}, \tag{10}$$

where coefficients A_1 and A_3 become zeros when the supporting layer has infinite thickness (model 2). Then one can derive the solutions for displacements and stresses in the transform domain:

$$\tilde{\tilde{u}} = ik(A_1(k,\omega)e^{R_L z} + A_2(k,\omega)e^{-R_L z}) + R_T(A_3(k,\omega)e^{R_T z} - A_4(k,\omega)e^{-R_T z}) \tag{11a}$$

$$\tilde{\tilde{w}} = R_L(A_1(k,\omega)e^{R_L z} - A_2(k,\omega)e^{-R_L z}) - ik(A_3(k,\omega)e^{R_T z} + A_4(k,\omega)e^{-R_T z}) \tag{11b}$$

$$\begin{aligned}\tilde{\tilde{\sigma}}_{zz} = [(\tilde{\tilde{\lambda}} + 2\tilde{\tilde{\mu}})(R_L)^2 - \tilde{\tilde{\lambda}}k^2][A_1(k,\omega)e^{R_L z} + A_2(k,\omega)e^{-R_L z}] - \\ -2ik\tilde{\tilde{\mu}}R_T[A_3(k,\omega)e^{R_T z} - A_4(k,\omega)e^{-R_T z}]\end{aligned} \tag{11c}$$

and hence, by using boundary conditions, one obtains the system of algebraic equations with respect to A_i that can be solved accordingly to the Cramer's rule:

$$A_j(k,\omega) = (\int_{-\infty}^{+\infty} P(t)e^{i(\omega - kV)t}dt)D_j(k,\omega)/D(k,\omega) \tag{12}$$

with D and D_j the associated determinants. The solution for vertical displacement is represented by the equation:

$$\tilde{\tilde{w}}(k,0,\omega) = \tilde{\tilde{w}}_0(k,\omega)\int_{-\infty}^{+\infty} P(t)e^{i(\omega - kV)t}dt \tag{13}$$

where $\tilde{\tilde{w}}_0(k,\omega) = (R_L(D_1 - D_2) - ik(D_3 + D_4))/D$ for model 1 and $\tilde{\tilde{w}}_0(k,\omega) = (-R_L D_2 - ikD_4)/D$ for model 2. Hence, by the Fourier transform (8), one can obtain the integral form of solution for the displacements at the surface:

$$w(0,0,t) = \frac{1}{4\pi^2}\int_{-\infty}^{+\infty}\int_{-\infty}^{+\infty}\tilde{\tilde{w}}_0(k,\omega)(\int_{-\infty}^{+\infty}P(t_1)e^{i(\omega - kV)t_1}dt_1)e^{-i\omega t}dkd\omega. \tag{14}$$

When the moving load is harmonically varying in time with the load frequency Ω, $P(t) = P_0\cos(\Omega t)$, formula (14) takes the following form:

$$w(0,0,t) = \frac{P_0}{4\pi}\int_{-\infty}^{+\infty}[\tilde{\tilde{w}}_0(k,kV - \Omega)e^{-i(kV-\Omega)t} + \tilde{\tilde{w}}_0(k,kV + \Omega)e^{-i(kV+\Omega)t}]dk. \tag{15}$$

The case of $\Omega = 0$ can be treated as a load constant in time. For this type of load the integrand in (15) has a strong singularity that prevents direct numerical calculation of the vertical displacement for both models. Therefore, in this paper, the displacements for relatively low load frequency are derived in order to approximate the constant point load. Instead of classical numerical integration, the alternative method [10] based on wavelet approximation of the inverse Fourier transform is used for calculation of integral (15). This method was previously successfully applied for the solution of number problems related to ground born vibrations analysis and investigation of interactions of fast railway transportation with the environment [12, 15, 16]. This method is very efficient for the analysis of ground and beam vibrations generated by loads moving with velocities near critical values and relatively high or low load frequencies [12, 15]. The wavelet approach allows to analyse detailed features of dynamic systems which might be lost when using numerical integration.

The method adopted in this paper for calculation of integral (15) is based on wavelet expansion of functions in $L^2(\mathbf{R})$, with multiresolution coefficients $c_{n,k}$ and $d_{j,k}$ obtained by using specially constructed wavelet filters:

$$f(x) = \sum_{k=-\infty}^{+\infty}2^{n/2}c_{n,k}\Phi(2^n x - k) + \sum_{j=n}^{\infty}\sum_{k=-\infty}^{+\infty}2^{j/2}d_{j,k}\Psi(2^j x - k). \tag{16}$$

Φ and Ψ are the scaling function and the wavelet function, respectively, derived in this paper by using coiflet filter p_k listed in Appendix. The average value of these coefficients ($M_2 = \sum_{k=0}^{M_1} k p_k$) differs from any integer and therefore allows to take into account all terms of approximating sequence (16), as opposed to coiflet filters used in previous publications [12, 15, 16]. In those cases, another singularity appeared in wavelet formulas and due to that fact, an additional approximating procedure was needed in order to eliminate troublesome terms. This modified system of coiflets improved the approximation accuracy and eliminated doubts related to analytical nature of the used sequences.

For the coiflets, the approximating formula (16) takes the following form:

$$f(x) = \lim_{n\to\infty} f_n(x) = \lim_{n\to\infty} \frac{2^{-n-2}}{\pi} \prod_{j=1}^{j_0} \left(\sum_{k=0}^{M_1} p_k e^{ikx/2^{j+n}}\right) \sum_{k=k_{\min}}^{k_{\max}} \tilde{f}((k+M_2)2^{-n}) e^{ixk2^{-n}} . \qquad (17)$$

M_1, M_2, j_0 are integers and $k_{\min}(n) = \omega_{\min} 2^n - 16$, $k_{\max}(n) = \omega_{\max} 2^n - 1$ define the interval $[\omega_{\min}, \omega_{\max}]$ covering the set of variable ω in transform domain which has important meaning for the nature of original function. Formula (17) can be used for derivation of original function f from its Fourier transform $\tilde{f}$, with significantly large n. Usually, it is sufficient to assume $n = 4$ and f_4 almost coincides with the original function. Nevertheless, the term f_{17} is used in this paper, due to the fact that considered, relatively low, load frequencies shows strong sensitivity of the system for its dynamic changes. Numerical simulations show that for $n > 16$ the sequence (17) stabilises and further terms do not differ significantly. One should note that a similar procedure can be applied for a wide spectrum of daublets and coiflets filters which were specially constructed for numerical applications. These carefully considered and modified, if needed, systems of coefficients give approximation with appropriate accuracy depending on the nature of the analysed systems.

4. Wavelet evaluation of displacements – numerical examples

The following system of parameters [4, 6, 12, 15, 16] is considered for parametric analysis: Young's modulus $E = 3 \cdot 10^7\ \mathrm{N/m^2}$; the mass density $\rho = 1700\ \mathrm{kg/m^3}$; $\mu^* = \lambda^* = 3 \cdot 10^4\ \mathrm{kg/ms}$ and Poisson's ratio $\nu = 1/3$ for the soil; the mass density $\rho_B / a = 3 \cdot 10^4\ \mathrm{kg/m^2}$; the bending stiffness $EI / a = 10^9\ \mathrm{Nm}$, the width in y direction $a = 4\,\mathrm{m}$ and the vertical point load $P_0 = 5 \cdot 10^4\ \mathrm{N}$ for the beam. The harmonic load is moving with three different velocities: $35\,\mathrm{m/s} \approx 0.46 \cdot c_R$, $65\,\mathrm{m/s} \approx 0.86 \cdot c_R$, $80\,\mathrm{m/s} \approx 1.05 \cdot c_R \approx 0.98 \cdot c_T$. These velocities allow to highlight some features of the system response for harmonic and constant loads. The values $c_R \approx 76\,\mathrm{m/s}$ and $c_T \approx 82\,\mathrm{m/s}$ are the Rayleigh velocity and the velocity of the shear waves in the soil, respectively. The thickness of the soil in model 1 is assumed to be $10\,\mathrm{m}$ and $10^4\,\mathrm{m}$, and those cases are compared with model 2. The load frequency $f_\Omega = \Omega / 2\pi$ is equal to $0.1/2\pi\,\mathrm{Hz}$, $0.01/2\pi\,\mathrm{Hz}$ and $10^{-10}/2\pi\,\mathrm{Hz}$ for the representation of the estimated constant load [4].

Numerical simulations show (Fig. 3) that vertical displacement for the constant load can be approximated by the harmonic one with relatively low load frequency. One can show that the response characteristics stabilises when the frequency load increases below $10^{-6}\,\mathrm{Hz}$ for the considered system. Therefore the value $\Omega = 10^{-10}$ of the frequency for the harmonic load is considered in parametric analysis for the investigation of the load constant in time.

Figures 4 and 5, show plots of the vertical displacements for different sub-critical velocities and both considered models. One can observe that even relatively high thickness of the supporting layer in model 1 does not give a good approximation of the more realistic model when the soil under the beam

is a half space (Figs. 1 and 2), especially for high velocities near critical values (Fig. 5). Therefore one should analyse very carefully models with finite supporting layer [4] because complex dynamic variations of the system can give wrong results when applying this assumption. However the waves' reflections might influence obtained results for this model, the propagation of reflected waves can be negligible due to viscoelastic properties of layer and its appropriately chosen thickness for the approximating procedure.

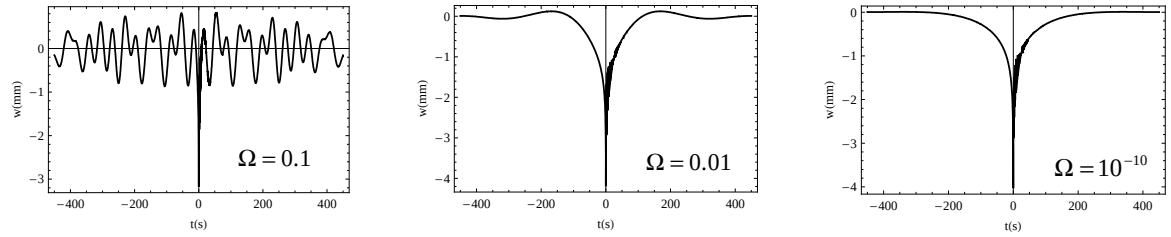

Figure 3: The vertical displacement for model 1 and $h = 10^4\,\mathrm{m}$.

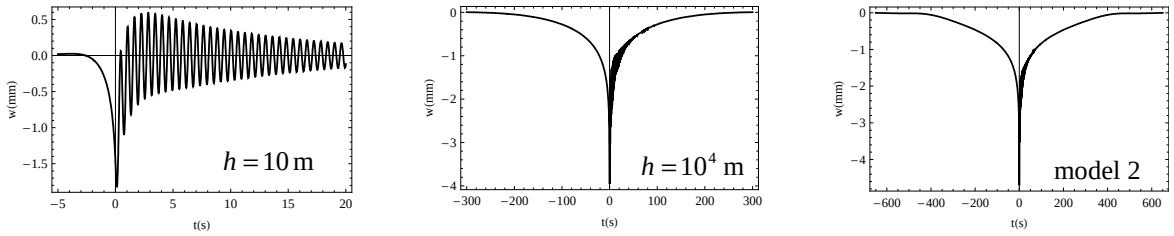

Figure 4: The vertical displacement for the velocity $V = 35\,\mathrm{m/s}$.

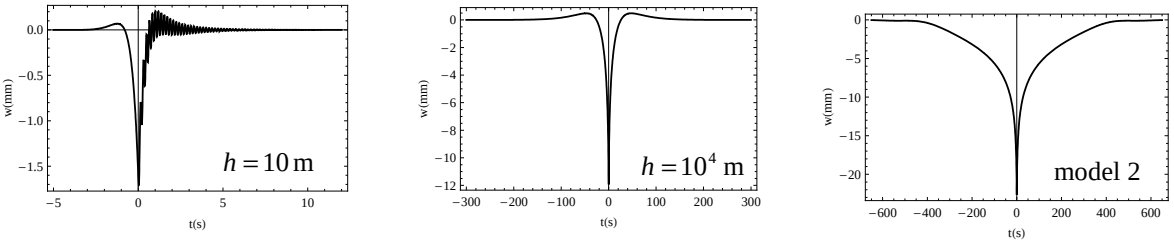

Figure 5: The vertical displacement for the velocity $V = 80\,\mathrm{m/s}$.

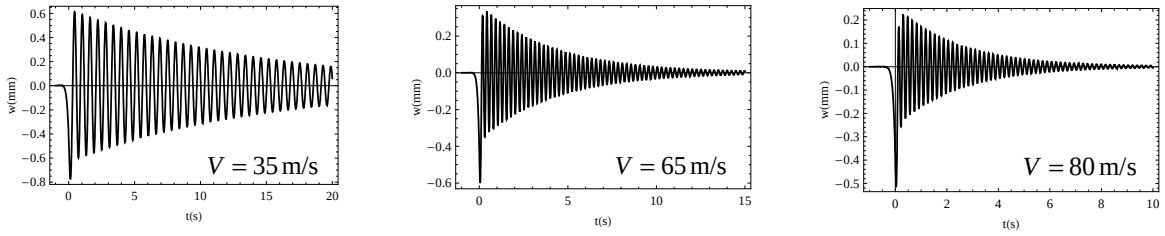

Figure 6: The vertical displacement for $h = 10\,\mathrm{m}$.

Figure 6 shows that the maximum amplitude of vertical vibrations decreases for higher velocities when the frequency load is equal to $\Omega = 10^{-10}$ which means that the assumption of the thickness $h = 10\,\mathrm{m}$ for the supporting layer is not realistic and leads to wrong results. This tendency is reversed when the value h increases (Fig. 7) and these correct observations of the influence of velocity on train

induced vibrations are confirmed by the analysis of more realistic model 2 (Fig. 8) and by the theory [3, 4, 6, 7, 12]. The wavelet method adopted in this paper for the derivation of vertical displacements allows further detailed analysis of the system, especially in the area of high velocities and the point load constant in time.

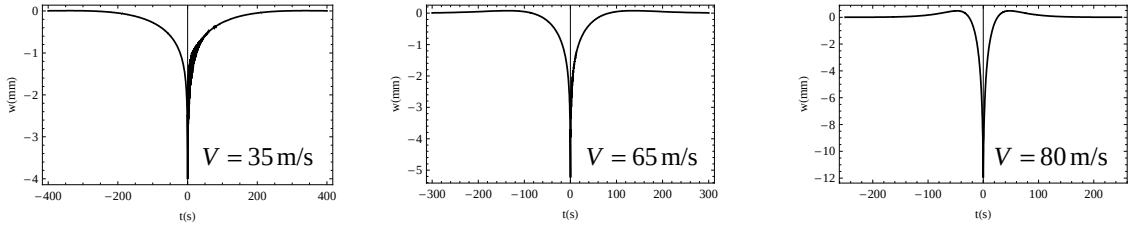

Figure 7: The vertical displacement for $h = 10^4$ m.

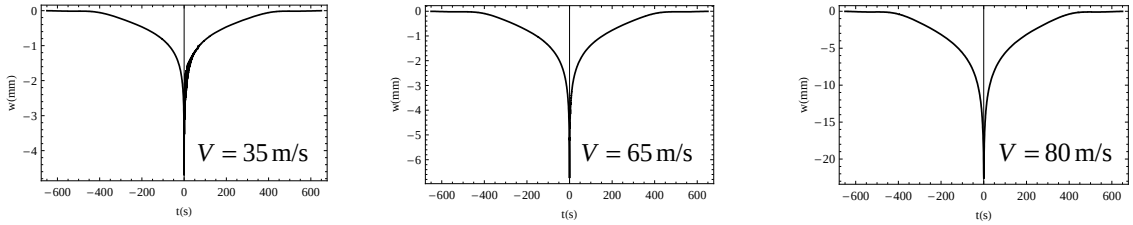

Figure 8: The vertical displacement for model 2.

The maximum amplitude derived by using the coiflet based wavelet approximation for a wide range of velocities shows that critical value of velocity for the constant load can be estimated around $80\,\mathrm{m/s}$ for model 2 (Fig. 9). One can observe that the vibrations can reach the relatively high level of $40\,\mathrm{mm}$ when the constant load moves with velocity near critical value.

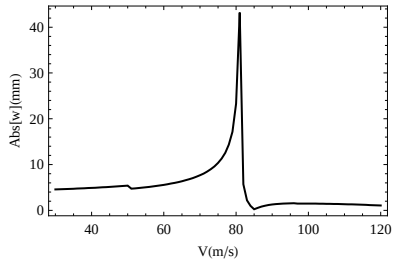

Figure 9: Critical velocity for model 2 and constant load – the maximum of vertical displacement.

5. Conclusions

The problem of viscoelastic soil vibrations generated by a load moving along a beam resting on the surface was analysed in two cases: with finite thickness of supporting layer and with half space under the beam. A special wavelet method was adopted for the derivation of vertical displacements at the surface. This method allowed to carry out the analysis in the area of high velocities and low frequencies leading to the approximation of the point load constant in time. The applied estimation allowed to alleviate the problem of singularities appearing in the integrated formulas when the constant load was considered. The modified coiflets filter improved the accuracy of wavelet approximation compared to previously published results. The parametric analysis of the system was carried out depending on a number of factors, e.g. the thickness of supporting layer and the velocity of moving load and the critical velocity was numerically estimated for the constant load and a half space

under the beam. The analysis of this system can be extended by using the wavelet approach for more complex situations.

Appendix

The following set of coiflets is used for numerical calculations performed in this article:

{0.003401479882015607, -0.004130806329954543, -0.03536170269249431, 0.0574776710426499 3, 0.3843902644404712, 0.5358632409346619, 0.1908760013178301, -0.1321131305836887, -0.05295999083912471, 0.05813917906468963, 0.00975811187504831, -0.01825628044991493, 0.0002608645070967113, 0.00327048515783943, -0.0003823627249285679, -0.0002646325745805278, 0.000017334234085592, 0.0000142737382977 0887}.

References

[1] Hermsworth B., (2000). Reducing groundborne vibrations: state of the art study. Journal of Sound and Vibration, 231(3), 703-709.

[2] Chen Y.H., Huang Y.H., (2003). Dynamic characteristics of infinite and finite railways to moving load. Journal of Engineering in Mechanics, 129(9), 987 – 995.

[3] Fryba L., (1999). Vibrations of Solids and Structures under Moving Loads. Thomas Telford Ltd., London.

[4] Metrikine A.V., Vrouwenvelder A.C.W.M, (2000). Surface ground vibration due to a moving train in a tunnel: two – dimensional model. Journal of Sound and Vibration, 234(1), 43-66.

[5] Dieterman H.A., Metrikine A., (1996). The equivalent stiffness of a half space interacting with a beam. Critical velocities of a moving load along the beam. European Journal of Mechanics A/Solids, 15, 67-90.

[6] Krylov V.V. (ed.), (2001). Noise and Vibrations from High-Speed Trains. Thomas Telford Ltd, London.

[7] Madshus C., Kaynia A.M., (2000). High speed railway lines on soft ground: dynamic behaviour at critical train speed. Journal of Sound and Vibration 231(3), 689-701.

[8] Dieterman H.A., Metrikine A., (1996). The equivalent stiffness of a half space interacting with a beam. Critical velocities of a moving load along the beam. European Journal of Mechanics A/Solids 15, 67-90.

[9] Kononov A.V., Wolfert R.A.M., (2000). Load motion along a beam on a viscoelastic half-space. European Journal of Mechanics and Solids 19, 361-371.

[10] Wang J., Zhou Y., Gao H., (2003). Computation of the Laplace inverse transform by application of the wavelet theory. Communications in Numerical Methods in Engineering 19, 959-975.

[11] Beylkin G., Coifman R., Rokhlin V., (1991). Fast wavelet transforms and numerical algorithms. Communications on Pure and Applied Mathematics, 44, 141-183.

[12] Koziol P., Mares C., Esat I., (2008). Wavelet approach to vibratory analysis of surface due to a load moving in the layer. International Journal of Solids and Structures 45, 2140-2159.

[13] Dieterman H.A., Metrikine A., (1997). Critical velocities of a harmonic load moving uniformly along an elastic layer. Transaction of the ASME Journal of Applied Mechanics 64, 596-600.

[14] Achenbach J.D., (1984). Wave Propagation in Elastic Solids, Elsevier, Amsterdam.

[15] Koziol P., Mares C., Esat I., (2007). Analysis of surface vibrations generated by underground fast train. International Conference on Engineering Dynamics, Carvoeiro, Algarve, Portugal, 16-18 April 2007.

[16] Koziol P., Mares C., Esat I., (2008). Wavelet analysis of a solid vibration due to a load moving along a beam resting on a surface. International Conference on Noise and Vibration Engineering, Leuven, ISMA2008.